IEEE Access
Multidisciplinary | Rapid Review | Open Access Journal

Received September 11, 2017, accepted September 29, 2017, date of publication October 18, 2017,
date of current version November 7, 2017.

Digital Object Identifier 10.1109/ACCESS.2017.2760201

Research on Automatic Parking Systems Based on Parking Scene Recognition

SHIDIAN MA[1], HAOBIN JIANG[1,2], MU HAN[3], JU XIE[2], AND CHENXU LI[2]

[1]Automotive Engineering Research Institute, Jiangsu University, Zhenjiang 212013, China
[2]School of Automotive and Traffic Engineering, Jiangsu University, Zhenjiang 212013, China
[3]School of Computer Science and Communication Engineering, Jiangsu University, Zhenjiang 212013, China

Corresponding author: Mu Han (hanmu@ujs.edu.cn)

This work was supported in part by the Natural Science Fund for Colleges and Universities in Jiangsu Province under Grant 12KJD580002 and Grant 16KJA580001 and in part by the National Natural Science Foundation of China under Grant 51675235.

ABSTRACT As a key component of intelligent vehicle technology, automatic parking technology has become a popular research topic. Automatic parking technology can complete parking operations safely and quickly without a driver and can improve driving comfort, while greatly reducing the probability of parking accidents. An automatic parking system based on parking scene recognition is proposed in this paper to resolve the following issues with existing automatic parking systems: parking scene recognition methods are less intelligent, vehicle control has a low degree of automation, and the research scope is limited to traditional fuel vehicles. To increase the utilization of parking spaces and parking convenience, machine vision and pattern recognition techniques are introduced to intelligently recognize a vertical parking scenario, plan a reasonable parking path, develop a path tracking control strategy to improve the vehicle control automation, and explore a highly intelligent automatic parking technology roadmap. This paper gives three key aspects of system solutions for an automatic parking system based on parking scene recognition: parking scene recognition, parking path planning, and path tracking and control.

INDEX TERMS Intelligent vehicles, automatic parking system, electric vehicles, parking scene recognition, path planning, non-smooth control, path tracking.

I. INTRODUCTION

With the rapidly increasing urban population and improvements in living standards, the number of vehicles has increased dramatically. The rapid increase in urban car ownership not only increases the burden of urban traffic but also exacerbates the problem of insufficient parking spaces. The increased driving distance in the parking process increases energy consumption and exacerbates parking difficulties, which increasing the number of minor accidents, such as scuffing and collisions [1], [2]. At present, intelligent vehicles are the main development trend of the automotive industry and is the research focus of major domestic and foreign automobile manufacturers and research institutions. As a key component of intelligent vehicle technology, automatic parking technology has become a popular research topic. Automatic parking technology completes parking operations safely and quickly without a driver and can effectively improve driving comfort while greatly reducing the probability of accidents during parking. In addition, the popularization of automatic parking technology can promote the development of automatic and intelligent vehicles [3]–[6].

At present, there are two main research methods for studying automatic parking systems: the research methods based on ultrasonic sensors and those based on visual sensors [7].

Research on automatic parking systems based on ultrasonic sensors was developed relatively early. At present, ultrasonic sensors still play a vital role in the development of automatic parking systems. In early 1989, Derrick and Bernard began to study parking technology and published their research results in the field of parking [8]. Subsequently, Seong Gon and Bart Kosko conducted a study on parking control methods based on the fuzzy control theory [9]. Holve et al. achieved the automatic parking function of a model car based on the fuzzy rule control method [10]. Inoue *et al.* [11] designed an automatic parking motion control algorithm based on the constraints of a parking space and vehicle kinematics.

With the rapid development of image processing technology, some experts in the field of parking have begun to apply image processing technology to automatic parking systems. Ozkul *et al.* [12] studied a fuzzy control automatic parking assist system based on visual information in 2008.

Toyota introduced the Lexus LS460L, which was equipped with an intelligent parking assist system, in 2010 [13]; this vehicle model uses a camera to collect spatial information from behind the vehicle and has an auxiliary trend line function. The Valeo company released a new generation automatic parking system called Valet Park4U in 2013 [14].

The intelligent recognition of parking spaces is also related to machine vision and target detection and recognition technology. With the rapid development of intelligent transportation technology, vehicle detection and recognition technology has become a popular research topic that has been unprecedentedly applied in the field of vehicle detection and recognition [15]. Most of the existing methods are based on vehicle appearance characteristics. J. Ferryman used a three-dimensional vehicle model to match an input vehicle image [16]. The algorithm output is the result of the recognition and vehicle orientation. V. Petrovic proposed a recognition method that involves normalizing the corresponding regions of a vehicle and matching the extracted regional eigenvalues [17]. L. Dlagnekov proposed a vehicle recognition algorithm that uses the scale-invariant feature transform (SIFT) method to extract vehicle tail features [18]. T. Kato proposed a recognition method based on the multi-clustered modified quadratic discriminant function [19].

Existing automatic parking systems have two major problems. First, the parking scene recognition methods are less intelligent, and there are more requirements and restrictions on the parking spaces. Second, vehicle control has a low degree of automation. In addition to steering, existing parking systems require the driver to control the speed, gear and brake. In this paper, the advantages of ultrasonic sensor ranging and machine vision target detection and identification are combined to improve both the parking scene recognition of automatic parking systems and the utilization rate of parking spaces. Moreover, electric vehicle speed can be controlled by a voltage signal to automatically control parking speed and to coordinate vehicle speed and steering speed. This advantage is used to improve the effect of path following, to increase the intelligence of automatic parking technology and to enhance parking convenience.

This paper is organized as follows:

First, the parking scene recognition methods are studied. To begin, several samples are used to train the AdaBoost vehicle detector, and a transplant test is conducted. Then, red taillights are identified by the color model algorithm. Finally, the parking orientation of the vehicle is obtained.

Second, by analyzing the working principle of the automatic parking system, a parking scene model is established. To achieve practical application of vertical parking, the parking movement model and parking movement constraints are fully analyzed, and a reasonable and feasible vertical parking path planning program is proposed. This program provides a basis for the following steering wheel control and path adjustment for parking.

Third, to reflect vehicle movement correctly and accurately, a path tracking controller for automatic parking based on the vehicle dynamics model is designed to control the planning route and improve parking accuracy.

II. VERTICAL PARKING SCENE RECOGNITION

When using an automatic parking system to find a parking space, the most common method is to detect the width and depth of a parking space using ultrasonic sensors. To ensure that the doors on both sides of a vehicle can be opened normally, the system usually sets the width of the target parking space to be at least 70∼80 cm greater than the width of the car body. When a relatively narrow open parking space is detected, the system will recognize that the parking space is not suitable, resulting in wasted parking space. In this case, as long as the width of the parking space is greater than the minimum width of the requested parking space, a narrow parking space can still be used via the recognition of vertical parking scenes, reasonable planning of the parking path and adjustment of the final parking position. The required criteria are that the limited space will not affect the car doors and that the driver side door of all vehicles involved can be opened normally.

The purpose of this chapter is to achieve the recognition of vertical parking scenes, including the measurement of a parking space using ultrasonic radar sensors and the recognition of the parking orientations of the vehicles on both sides of an idle parking space using a visual sensor. At present, the use of ultrasonic sensors is the most common automatic parking technique, which we will not explore in this article. This chapter focuses on recognizing the orientation of parked vehicles by a visual sensor. The specific procedure detects vehicles and identifies red taillights in pictures. First, the system detects whether a vehicle exists in the picture taken by the visual sensor. Second, the system identifies red taillights in the pictures that contain a vehicle. Finally, the system determines the vehicle orientations in the vertical parking spaces on both sides of the target parking space.

A. VEHICLE DETECTION

Target detection is also called target extraction, and its purpose is to identify the required information from a picture. Target detection specifically refers to retrieving information from input pictures by a specific algorithm and checking whether the input pictures contain the target information. If a retrieval target exists, the target area will be marked. Vehicle detection is a kind of target detection. It is a popular research direction for machine vision and has been widely used for intelligent transportation, intelligent monitoring and military target detection.

1) APPLICATION OF THE AdaBoost ALGORITHM

In 2001, Viola and Jones proposed the AdaBoost algorithm based on machine learning to construct a face detection classifier [20]. The experimental results show that the method has good applicability. Because of the high detection speed and recognition accuracy, the machine recognition method based on the AdaBoost algorithm has become a popular research

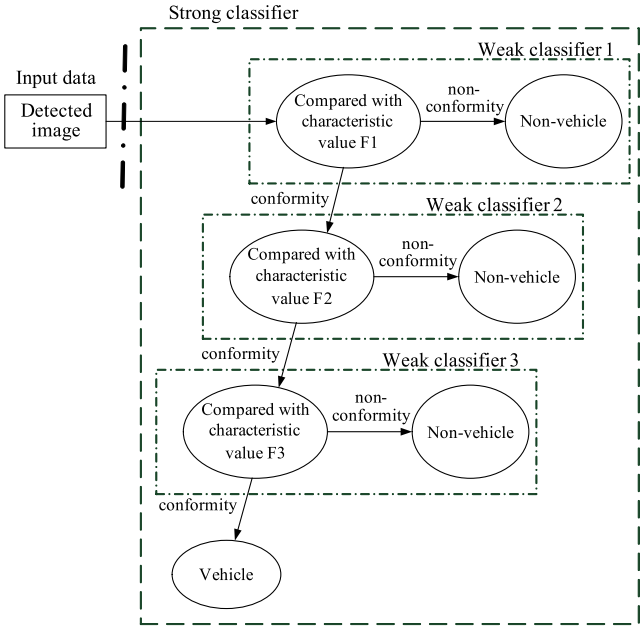

FIGURE 1. Strong classifier of the multilayer cascade.

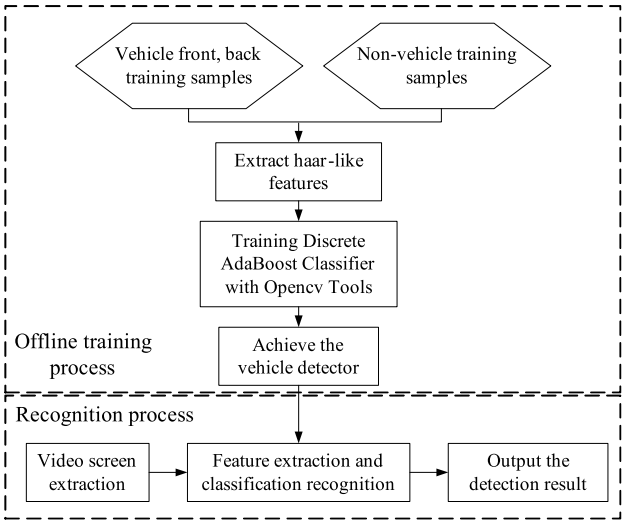

FIGURE 2. Process of the vehicle detection algorithm.

FIGURE 3. Correct vehicle areas obtained via detection.

topic in target detection. The basic principle of the AdaBoost algorithm is to construct a strong classifier cascaded by some weak classifiers based on Harr feature extraction. The multilevel strong classifier trained in this paper is cascaded by three weak classifiers, as shown in Figure 1. According to the successful application of face detection based on the AdaBoost algorithm, the algorithm is applied to the detection of vehicle orientation. The flow diagram of the detection algorithm is shown in Figure 2.

We collect 550 pictures of the front section of vehicles and 550 pictures of the back section of vehicles and use an image processing software to crop the collected pictures. We crop out 400 front and back area images. The cropped regions are grayscale processed and compressed into a pixel format of 28×12. The remaining pictures are used to test the recognition of the detector designed in this paper.

2) EXPERIMENTAL RESULT

The vehicle detector mentioned above is installed onto the QS-PTE9 video image processing development board. Then, the vehicle area is detected in the video images collected by the camera. Figure 3 shows the correctly detected vehicle areas, which are indicated by the red rectangles in the figure.

3) PERFORMANCE OF THE VEHICLE DETECTOR

a) Detection rate D_c: the number of correctly detected vehicle areas / the total number of vehicle areas included in the pictures. This variable reflects the ability of the vehicle detector to identify the target area. The higher detection rate indicates that the trained vehicle detector in this paper is more effective in recognizing vehicle areas.

b) Error detection rate D_m: the number of erroneously detected vehicle areas / the total number of vehicle areas included in the pictures. This variable reflects the ability of the vehicle detector to exclude non-target areas. The lower detection rate indicates that the trained vehicle detector in this paper is more effective in excluding non-vehicle areas.

c) Detection speed V_d: The detection speed indicates the time it takes to successfully detect the presence of a vehicle in a picture when using a detector to detect the input picture.

d) Robustness: Robustness indicates the adaptability of the vehicle detector when the external environment changes. The same car is placed under different lighting conditions or with different background scenes, and pictures are taken from the same point of view. We use the vehicle detector trained in this paper to identify and detect the group of pictures and determine whether the detection rate D_c, the error detection rate D_m and the detection speed V_d change considerable.

TABLE 1. Partial performance indexes of the vehicle detector.

	Detection rate D_c	Error detection rate D_m
Percent (%)	$\frac{563}{600} = 93.83\%$	$\frac{52}{617} = 8.43\%$

The detection performance of the vehicle detector trained in this paper is tested using 600 pictures that are not used for positive sample training and that contain the vehicle target area. These images are input into the vehicle detector, and the detection results are calculated and analyzed. The results show that the total number of detected vehicle areas is 617, where the number of correctly detected vehicle areas is 563 and the number of erroneously detected vehicle areas is 52. The detection rate and error detection rate of the vehicle detector trained in this paper are shown in Table 1.

In terms of detection speed, the detector requires approximately 0.1 s to successfully detect the presence of a vehicle area when a picture of 1024 × 800 pixels is input, which meets the requirements of real-time detection. In terms of robustness, the lighting conditions and the background environment have little influence on the detector, but the angle of the vehicle image in the pictures does affect the performance. The detector can identify only the front and back sections of vehicles in the images when the horizontal rotation viewing angle is within 20° and the up and down viewing angle is within 20°. Therefore, the position and angle of the camera need to be calibrated for a real vehicle test.

B. VEHICLE TAILLIGHT IDENTIFICATION

In this study, the orientation of a parked vehicle in a vertical parking space needs to be recognized based on the detected vehicle areas presented in the preceding subsection. All vehicles have red taillights, which are a significant regional feature that can be used to distinguish the front and back of a vehicle. This section uses the unique color information of red taillights to identify and locate the red taillights based on the detected vehicle area discussed above. Thus, the orientation of a parked vehicle in a vertical parking space can be recognized.

1) CHARACTERISTIC ANALYSIS OF TAILLIGHTS

First, the characteristics of vehicle taillights are analyzed:

a) *Color characteristics of taillights*: Most vehicle taillights include materials of several different colors, but they must contain very eye-catching red brake lights that occupy a large area.

b) *Distribution characteristics of taillights*: Vehicle taillights always appear in pairs and are symmetrically distributed on the left and right sides of the rear of vehicles.

Because the symmetrical distribution of red taillights is easier to distinguish and detect than other body features, this paper uses the taillights as the object of identification.

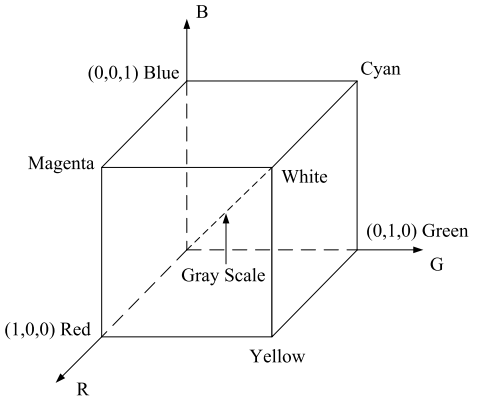

FIGURE 4. RGB color space cube.

2) SELECTION OF COLOR MODELS

A color model, also known as a color space or color system, is a subset of visible light in a three-dimensional color space. It contains all the colors of a color field, each of which is represented by a single point. The main purpose of a color model is to simplify the color specification in an acceptable manner under certain criteria. Its essence is the specification of the coordinate system and subspace. Most of the color models used today are hardware-oriented or application-oriented [21]. In practical applications, the RGB model is the most commonly used color model in digital image processing and is mainly used for color monitors and color video cameras. The HSI model can decompose an image into color and gray information and is more in line with human description and interpretation of color. Therefore, it is more suitable for gray processing technology. In addition, there are many other color models that are used in different areas. The following is a brief introduction to the three color space models applied in this paper.

a: RGB COLOR SPACE MODEL

The RGB color space model is usually represented by a unit cube, as shown in Figure 4. All R, G, and B values are selected in the range [0,1]. Along the cube's main diagonal, the intensities of the primary colors are equal and range from dark to bright white, that is, different gray values. In the RGB color space model, different colors are taken at different positions of the cube area and can be represented as vectors from the origin. There is a high degree of correlation among the components of the RGB space. It is difficult to achieve the desired results by using these three components directly, but the RGB color space model can provide some valuable information. Therefore, we can use the properties of the RGB model to select the red area of a vehicle taillight, as shown in the following formula.

$$\text{RedArea} = (R > B)\&(R > G)(\text{abs}(B - G) < 20) \quad (1)$$

b: HSI COLOR SPACE MODEL

The HSI color space is based on the human visual system of hue, saturation and brightness and is used to describe color.

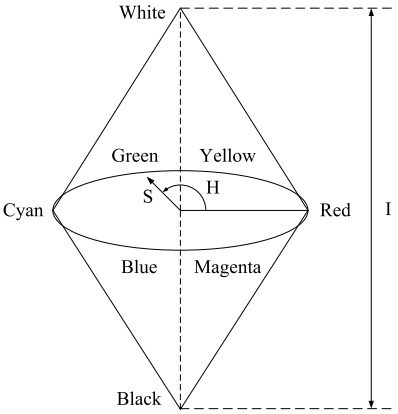

FIGURE 5. HSI color space cone.

This model is more focused on showing color that conforms to human visual characteristics so that an image looks more natural and intuitive. The HSI color space can be described by the cone space model shown in Figure 5. This model clearly shows the trends of the hue, color saturation and brightness and can separate the I component of a color image from the color information [22].

Figure 5 clearly shows that in the HSI color space cone, the H component and the S component are closely related to the color information perceived by the person and that the I component is related to only the black and white information. To simplify the computational difficulty, we use only the H and S components in the HSI color space to segment the color region. Therefore, the red area of the vehicle taillight can be selected according to the following formula.

$$\text{RedArea} = (\text{H} > 20)\&(\text{S} > 0.3) \tag{2}$$

Although the HSI color space model is effective for color region segmentation, the number of computations needed to convert from the RGB space to the HSI space is very large. Therefore, this section uses only the HSI color space model as a supplementary model.

c: YC_bC_r COLOR SPACE MODEL

The YC_bC_r color model is commonly used in video images and digital images. Y represents the luminance information, and the color information is described and stored by the two chromatic components C_b and C_r. The chromatic components C_b and C_r are the coordinates of the blue component and the red component with respect to the reference value, respectively [23].

The YC_bC_r color space model is less affected by the brightness, that is, the chromatic components C_b and C_r are less correlated with the luminance component Y, and only the red taillight area is selected to be segmented, that is, the only information that is actually used is the chromatic component C_r. Therefore, we need to calculate only the chromatic component C_r, and the formula for converting from the RGB color space model to the YC_bC_r color space model can be simplified as follows.

$$C_r = 128 + \begin{bmatrix} 112.000 & -93.786 & -18.214 \end{bmatrix} \begin{bmatrix} R \\ G \\ B \end{bmatrix} \tag{3}$$

The simplification of the calculation greatly reduces the time spent transforming the space model. In addition, with respect to the actual effect of color segmentation, the color segmentation effect of the YC_bC_r color space is better than that of the HSI color space.

Considering the advantages and disadvantages of the above three color space models, the red region of a vehicle taillight is segmented using a color space model that combines the RGB color space model and the YC_bC_r color space model, while the HSI color space model is used as the supplementary segmentation scheme.

3) TAILLIGHT LOCALIZATION ALGORITHM

First, the input of the detected picture is prepared for pretreatment, which includes filter denoising and image smoothing. Then, the red region of the vehicle area in a picture is segmented using the combined RGB and YC_bC_r color space model. Finally, according to the distribution characteristics of the red taillights, the area of the red taillights is filtered out via the morphological method. If the region does not meet the conditions after completing the above steps, in accordance with the above steps, the HSI color space model is used to process the picture again to reduce the probability of missing the red taillights. The algorithm flowchart is shown in Figure 6.

4) EXPERIMENT AND RESULTS ANALYSIS

Some of the vehicle images identified by the vehicle detector are tested for red taillights. Some of the experimental results are as follows.

Although the algorithm cannot accurately identify the red taillight of a car with a red body, as shown in Figure 7(c), it can accurately identify the red taillight areas of cars with other body colors, as shown in Figure 7(a) and Figure 7(b).

III. MODELING AND ROUTE PLANNING FOR PARKING

Constructing a reasonable and effective vehicle movement model is a prerequisite for studying automatic parking control systems. Such a model not only determines the parking trajectory of a vehicle but also affects the complexity of the control system. Therefore, this chapter analyzes the architecture and working principle of the system and establishes a parking scene model based on the functional requirements and design constraints of the parking system. To achieve practical applications to vertical parking, this chapter analyzes the parking movement model and the restraint of the parking movement and proposes a reasonable and feasible path planning scheme for vertical parking to improve parking convenience and the utilization rate of parking spaces.

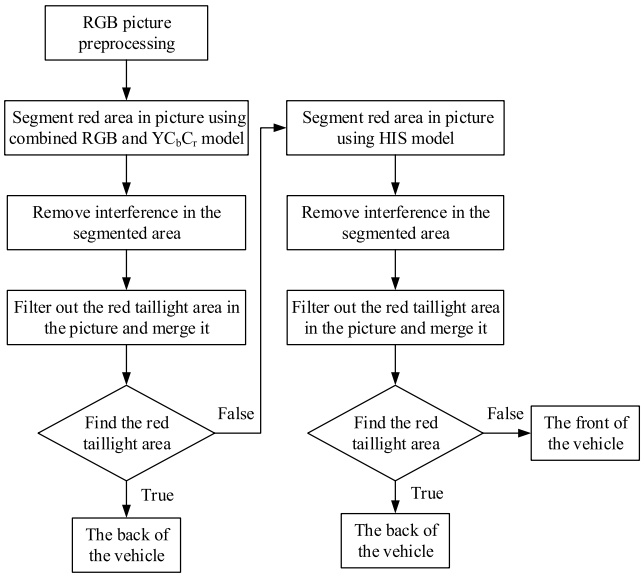

FIGURE 6. Algorithm flowchart for detecting the red taillight area.

FIGURE 7. Detection result of the red taillight area.

A. SYSTEM WORK PROCESS

An automatic parking system includes two programs: parallel parking and vertical parking. This paper studies the vertical parking system, and its complete process is described in the following.

First, a driver drives a car into a parking area and activates the automatic parking system, as shown in Figure 8, position A. In the process of looking for a parking space (from position A to position B), the visual information processing module and the ultrasonic module that measures lateral distance work simultaneously to identify the orientation of each parked vehicle and to measure the distances.

In the detection process, the vehicle drives through the parking area at a constant speed v. Because vehicles are parked on the left and right sides of the parking space, the distance detected by the ultrasonic sensors will jump when the sensor passes the edge of a vehicle body; this jump is used as the basis for judging the boundary of the parking space. By recording the time interval t of two jumps, the width of the parking space can be obtained by $l = v \times t$. At the same time, the visual sensors work to recognize the orientation of each parked vehicle.

According to the above information and the real-time speed data acquired by the vehicle running state acquisition module, the system will judge whether the current parking space satisfies the parking requirements. If the requirements are met,

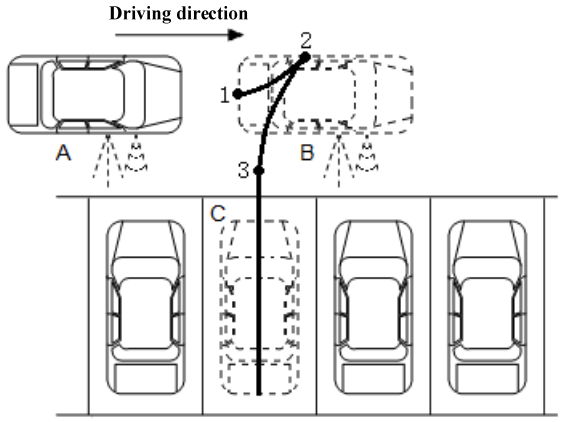

FIGURE 8. Vertical parking process diagram of an automatic parking system.

the system will send alerts regarding the available parking space to the driver along with parking tips, and the driver will confirm whether the parking space is accepted.

If the distance measured by the measurement module is greater than that required for conventional parking, that is, the parking width D $\geq$ body width d $+0.6$ m, the system determines that the space is a regular vertical parking space. In this case, the parking path is determined based on the information obtained by the ultrasonic measurement module. The information obtained by the visual processing module also plays a role in safety monitoring. If the distance measured by the ultrasonic measurement module is smaller than that required for conventional parking but greater than the minimum parking space requirement, that is, the vehicle body width d $+0.4$ m $\leq$ parking width D $<$ body width d $+0.6$ m, the system determines that the space is a narrow vertical parking space. In this case, the parking path is determined based on the information obtained by both the ultrasonic distance measurement module and the visual processing module.

Second, at position B in Figure 8, after the driver confirms the parking space, the system executes the parking process. During the parking process (from position B to position C), the control module plans the parking path based on the current parking space, vehicle distance information and the motion parameters of the vehicle. To prevent accidents during the parking process, the system detects the presence of obstacles around the vehicle using the distance measurement module. By coordinating the communication module, the EPS (Electric Power Steering) controller, the gear control unit, the speed control unit and the electronic brake, the system completes automatic coordination control of the vehicle, including the steering wheel rotation, gear selection, speed control and active braking, until the whole parking process is completed.

B. SYSTEM FUNCTIONAL REQUIREMENTS AND DESIGN CONSTRAINTS

1) ANALYSIS OF PARKING FUNCTION REQUIREMENT

According to the working process of automatic parking, it is necessary to store the envelope parameter information of the

vehicle and the minimum parking space dimensions in the control unit. In the system operation, the control unit must monitor the running state of the vehicle in real time and detect changes in the parking environment. When the detected parking space meets the parking requirement, that is, the size of the detected parking space is larger than the minimum size required for a parking space, the system will alert the driver. If the driver accepts the parking space, the system will switch to automatic parking mode, taking over the vehicle steering, automatic control parking speed, and vehicle gears and brakes, to complete the parking process.

The above analysis shows that the functional requirements of an automatic parking system are mainly as follows.

a) Detection of vehicle operating status: The real-time detection of vehicle speed is used to calculate the vehicle driving distance for the detection of vehicle travel trajectories, the detection of the length of a parking space, the collaborative control of the speed and steering wheel, and tracking of the preplanned path. The detection of the gear position is used to determine whether a vehicle is traveling forward or in reverse. The detection of the steering wheel speed and rotation angle is used to form the closed-loop control of the steering wheel and the speed.

b) Parking scene detection: The width and depth of a parking space are detected by the long-range ultrasonic radar sensor. The visual system of the moving vehicle is used to identify the orientation of parked vehicles. The short-range ultrasonic radar sensor is used to detect the presence of obstacles.

c) Vehicle steering control: The system should be able to turn the steering wheel automatically and return it to any angle and to adjust the angular velocity.

d) Vehicle gear control: The system should achieve automatic switching of the stalls at a particular location in the parking process.

e) Vehicle speed control: The system should achieve active control of the speed during the parking process and actively adjust the angular velocity of the steering wheel according to the current speed to achieve collaborative control of the speed and steering.

f) Active braking control: The system should achieve active braking control for when an emergency occurs or the parking process is completed.

g) Protection of the data stored in the control unit: The ECU internal settings data must be stored in nonvolatile storage.

2) EXPERIMENTAL VEHICLE PARAMETERS

In this paper, a pure electric vehicle is used as the experimental vehicle, and its specific parameters and symbols are shown in Table 2.

TABLE 2. Experimental vehicle parameters.

Parameter	Symbol	Value
Vehicle width (mm)	W	1540
Wheelbase (mm)	L	1765
Front track (mm)	L_{tf}	1345
Rear track (mm)	L_{tr}	1301
Front overhang (mm)	L_f	560
Rear overhang (mm)	L_r	480
Tire type		155/50 R14
Minimum turning radius (mm)	R_{min}	3780

3) DETERMINATION OF PARKING SPACE SIZE

The external parking environment is different in different parking areas. This paper focuses on the common vertical parking spaces. The sizes of the target parking spaces, as determined by the automatic parking system described in this paper, are formulated according to the vehicle system parameter settings, the relevant national regulations and the actual measurements of the parking spaces, as shown in Figure 9. From the measurement of the actual parameters of some common vertical parking spaces, it can be concluded that the parking depth is usually greater than 6.5 m and that the width is generally approximately 2.4 m.

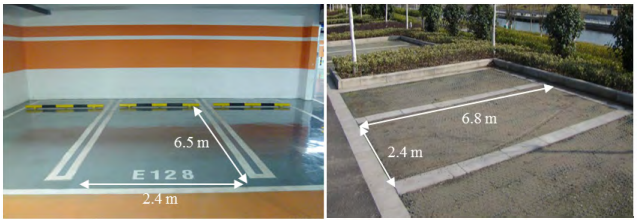

FIGURE 9. Common vertical parking spaces.

Because the experimental vehicle used in this article is a miniature electric vehicle, the body size of the vehicle is small. Therefore, experiments conducted using a conventional parking space size would not produce convincing results. To make the experimental results more convincing, the minimum vertical parking space required for the system is defined as having a depth of 4 m and a width of 2 m according to the experimental parameters of the vehicle and the provisions of the national standard for parking spaces. Furthermore, parking spaces with widths greater than 2.3 m are defined as conventional ones, while parking spaces with widths greater than 2.0 m but less than 2.3 m are defined as narrow ones.

The minimum vertical parking space required by this system is the size of the reference parking space, as shown in Figure 10.

C. ESTABLISHMENT OF THE KINEMATIC MODEL

Vehicle parking is a low-speed (usually below 5 km/h) movement process. When a vehicle's wheels roll at a low speed, it does not undergo lateral sliding; thus, the lateral force can be neglected, and there is no wheel side slip angle [24]. Therefore, in an actual application, the vehicle kinematic model is usually simplified, that is, the vehicle parking kinematics

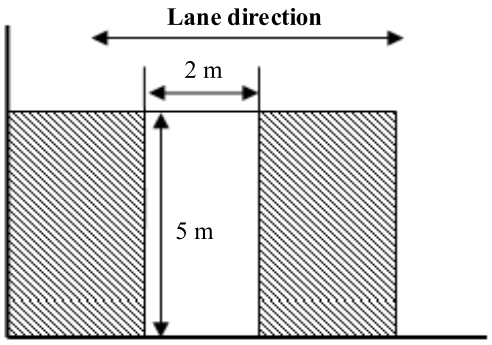

FIGURE 10. Reference size of a vertical parking space.

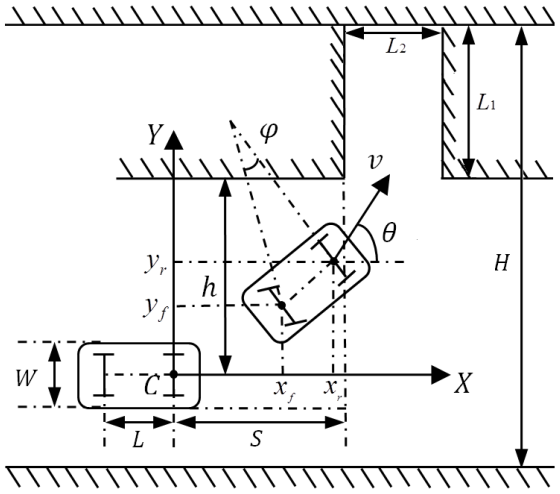

FIGURE 11. Simplified car model for parking.

model is established based on the vehicle kinematics model for the parking movement. This paper establishes the following simplified model for low-speed parking.

In this paper, the kinematics model of a vehicle is established, and the path planning method for an automatic parking system is studied based on this model. As shown in Figure 11, (x_r, y_r) are the midpoint coordinates of the rear axle of the vehicle, (x_f, y_f) are the midpoint coordinates of the vehicle's front axle, W is the width of the vehicle, H is the width of the road, L_1 and L_2 are the width and length of the target parking space, respectively, h is the distance between the midpoint of the rear axle and a lateral obstacle, S is the distance between the midpoint of the rear axle and the end of an obstacle in front of the target parking space, θ is the course angle of the vehicle, φ is the Ackerman angle, and the clockwise direction is positive.

Assuming that the vehicle rear wheel lateral velocity (vertical with respect to the wheel direction) is zero, the vehicle movement equation in the vertical direction can be obtained.

$$\dot{x}_r \cdot \sin\theta - \dot{y}_r \cdot \cos\theta = 0 \tag{4}$$

According to the Ackerman steering geometrical principle, the Ackerman angle φ in the process of car steering is approximately equal to the steering angle of the midpoint of the vehicle front axle, and the center angle of the front axle of the vehicle is approximately linearly proportional to the steering wheel angle γ [25].

$$\gamma = K \cdot \varphi \tag{5}$$

where K is the ratio constant.

The midpoint of the rear axle is taken as the origin; then, the coordinate system is established as shown in Figure 11. The positional relationship between the midpoints of the front and rear axles of the vehicle can be obtained from the figure.

$$\begin{cases} x_r = x_f + L \cdot \cos\theta \\ y_r = y_f + L \cdot \sin\theta \end{cases} \tag{6}$$

Formula (6) is differentiated to obtain the velocity relationship between the midpoints of the front and rear axles of the vehicle.

$$\begin{cases} \dot{x}_r = \dot{x}_f + L\dot{\theta} \cdot \cos\theta \\ \dot{y}_r = \dot{y}_f + L\dot{\theta} \cdot \sin\theta \end{cases} \tag{7}$$

Substituting (7) into (4), we can obtain the kinematics relationship of the vehicle.

$$\dot{x}_f \cdot \sin\theta - \dot{y}_f \cdot \cos\theta - L \cdot \dot{\theta} = 0 \tag{8}$$

In addition, at a certain moment during the parking process, the velocity of the midpoint of the front axle along the direction of the axis is

$$\begin{cases} \dot{x}_r = v \cdot \cos(\theta + \varphi) \\ \dot{y}_r = v \cdot \sin(\theta + \varphi) \end{cases} \tag{9}$$

Substituting (9) into (8), we can obtain

$$\dot{\theta} = -\frac{v \cdot \sin\varphi}{L} \tag{10}$$

Substituting (9) and (10) into (8), we can obtain the velocity of the midpoint of the front axle along the axis direction.

$$\begin{cases} \dot{x}_r = v \cdot \cos\theta\cos\varphi \\ \dot{y}_r = v \cdot \sin\theta\cos\varphi \end{cases} \tag{11}$$

Formulas (10) and (11) can be expressed as the kinematic equation of the vehicle.

$$\begin{cases} \dot{x}_r = v \cdot \cos\theta\cos\varphi \\ \dot{y}_r = v \cdot \sin\theta\cos\varphi \\ \dot{\theta} = -\dfrac{v \cdot \sin\varphi}{L} \end{cases} \tag{12}$$

Formula (12) is utilized to integrate time t, and we can obtain the trajectory equations of the midpoint of the rear axle.

$$\begin{cases} x_r(t) = -L \cdot \cot\theta \cdot \sin(\dfrac{v \cdot \sin\theta}{L} \cdot t) \\ y_r(t) = L \cdot \cot\theta \cdot \sin(\dfrac{v \cdot \sin\theta}{L} \cdot t) - L \cdot \cot\theta \\ x_r^2 + (y_r + L \cdot \cot\theta)^2 = (L \cdot \cot\theta)^2 \end{cases} \tag{13}$$

According to the geometric relation between the vehicle parameters and the coordinate positions in Figure 11, the trajectory equations of the four vehicle wheels and envelope points can be obtained. Thus, the actual trajectory of the vehicle during the whole parking process, from the starting point to the terminal point, can be calculated.

D. ANALYSIS OF PARKING SPACE CONSTRAINTS

The automatic parking process is conducted to find a smooth path curve for a vehicle attempting to park in a parking space. The path curve should not only satisfy the geometric characteristics of the movement of the vehicle but also ensure that the process does not result in an accident. Therefore, it is necessary to establish the corresponding constraints and plan the appropriate parking path curve so that the parking process is safe and accurate. This section analyzes the possible collision points in the parking process.

According to the planned parking path, namely, the rear parking trajectory function, the theoretical curvature ρ of the vehicle at an arbitrary point in the parking process can be given as

$$\rho = \frac{y''}{[1 + (y')^2]^{3/2}} \tag{14}$$

According to the relation of the Ackerman angle [26],

$$\tan\varphi = \frac{L}{R} \tag{15}$$

where L is the wheel base, R is the radius of the turning circle, and $R = 1 / \rho$.

According to (14) and (15), the Ackerman angle of the vehicle at an arbitrary point is

$$\varphi = \arctan\left(\frac{L \cdot y''}{[1 + (y')^2]^{3/2}}\right) \tag{16}$$

According to the coordinates of the midpoints of the rear axle and their mutual relationship, the trajectories of A, B, C and D can be obtained.

$$\begin{cases} x_A = x + (L_f + L) \cdot \cos\theta + \dfrac{W}{2} \cdot \sin\theta \\ y_A = y - (L_f + L) \cdot \sin\theta + \dfrac{W}{2} \cdot \cos\theta \end{cases} \tag{17}$$

$$\begin{cases} x_B = x + (L_f + L) \cdot \cos\theta - \dfrac{W}{2} \cdot \sin\theta \\ y_B = y - (L_f + L) \cdot \sin\theta - \dfrac{W}{2} \cdot \cos\theta \end{cases} \tag{18}$$

$$\begin{cases} x_C = x - \cos\theta - \dfrac{W}{2} \cdot \sin\theta \\ y_C = y + \sin\theta - \dfrac{W}{2} \cdot \cos\theta \end{cases} \tag{19}$$

$$\begin{cases} x_D = x - \cos\theta + \dfrac{W}{2} \cdot \sin\theta \\ y_D = y + \sin\theta + \dfrac{W}{2} \cdot \cos\theta \end{cases} \tag{20}$$

where L_f is the length of the front overhang and L_r is the length of the rear overhang.

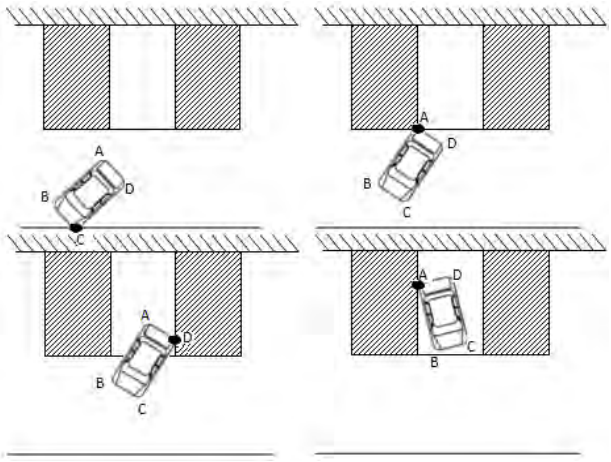

FIGURE 12. Possible vertical parking collisions.

As shown in Figure 12, there are four positions at which danger exists in the process of vertical parking.

a) Collision between the left front envelope point C of the vehicle and the left boundary of the roadway or a vehicle traveling along the left roadway during the parking process.

b) Collision between the right rear point A of the vehicle and an obstacle or parked vehicle on the right side of the available parking space during the parking process.

c) Collision between the left rear point B of the vehicle and an obstacle or parked vehicle on the left side of the available parking space during the parking process.

d) Collision between the right rear point A of the vehicle and an obstacle or parked vehicle on the right side of the available parking space after the vehicle is parked in the space.

To ensure that no collision occurs during the parking process, the trajectory function for vertical parking needs to satisfy the following conditions.

$$\begin{aligned} &\text{When } x_A \in [0, S], \quad y_A < h; \\ &\text{when } x_A \in [S, S + L_2], \quad y_A < h + L_1; \\ &\text{when } x_B \in [0, S], \quad y_B < h; \\ &\text{when } x_B \in [S, S + L_2], \quad y_B < h + L_1; \\ &\text{when } x \in [0, S + L_2], \quad y_C > h + L_1 - H; \\ &\text{and when } x = S + L_2, \quad y_D > h,\ y_D < h + L_1. \end{aligned}$$

The analysis of the kinematics constraints in the process of parking ensures the safety of the running vehicle during the parking and lays a foundation for the vehicle trajectory planning and path tracking in the parking process.

E. MODELING AND ANALYSIS OF VERTICAL PARKING SCENE

When parking in a vertical parking space, both sides of the vehicle often occupy part of the space in the middle empty parking space due to non-standard parking. This phenomenon

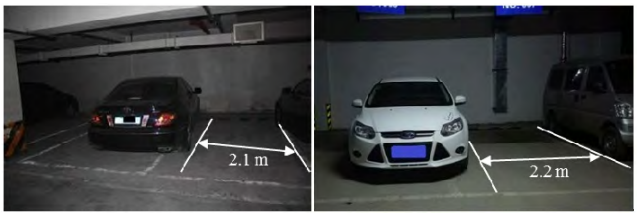

FIGURE 13. Non-standard parking in vertical parking spaces.

results in a smaller width of the middle empty parking space, as shown in Figure 13. The conventional parking spaces and narrow parking spaces described above are modeled below, and the characteristics of narrow parking spaces are analyzed.

1) CONVENTIONAL PARKING SPACES

The width of conventional parking spaces considered in this paper is at least 70 cm greater than the width of the vehicle body. This parking space scenario is common and simple. Because of the wider size of the parking spaces, a vehicle can achieve successful parking via vertical parking path planning.

2) NARROW PARKING SPACES

There are three kinds of available narrow parking spaces, and these parking spaces are modeled separately, as shown in Figure 14. The first special scene analyzed is as follows.

In the first scenario, the left vehicle is parked skew, and the right vehicle is parked with a deviation to the left such that it occupies part of the available parking space. As a result, the width of the middle parking space changes to 2.1 m. Both vehicles are parked such that the front of each vehicle is pointed towards the road; thus, their driver side doors both open to the left. If the moving vehicle parks in reverse in accordance with the conventional parking path, its driver side door should also open to the left. However, because of the narrow parking space, it will not be possible for the driver side door of this vehicle and that of the right vehicle to be opened.

In this case, if the moving vehicle parks head-on (instead of in reverse) and the final parking position is close to the right side of the left vehicle, the driver side door of this vehicle can be opened normally and does not affect the driver side door of the vehicle on the right, as shown in Figure 15. As a result, this problem can be solved by planning a reasonable parking path to improve the utilization of narrow parking spaces.

F. VERTICAL PARKING PATH PLANNING

The problem of vehicle parking path planning can be described as finding one or a set of continuous smooth curves between the starting point of the vehicle and the end point in the parking space. The curvature of this set of curves is not greater than $1 / R_{\min}$ ($R_{\min}$ is the minimum steering radius of the vehicle), and the trajectory of the vehicle along the path satisfies the analysis of the kinematics constraints. Parking paths are roughly divided into two types: backward

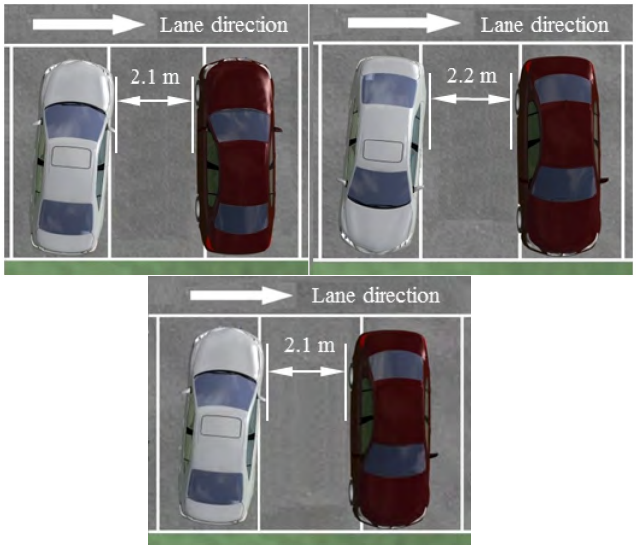

FIGURE 14. Three kinds of narrow parking scenarios.

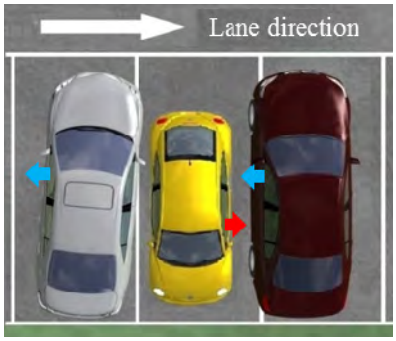

FIGURE 15. Reasonable use of narrow parking space.

paths and combination paths. In the vertical parking process, if the vehicle uses a two-segment backward path for parking, it needs to achieve a 90° heading angle change in the first segment of the path. This path requires a relatively large parking width. When the parking spaces are slightly narrow, the effect of parking is not ideal, or it is not possible to complete the parking process. Therefore, this section mainly studies the three-segment forward and backward combination path planning of vertical parking.

Via the analysis of vertical parking spaces, this paper proposes two kinds of parking path planning methods: a three-segment path for backing into parking spaces and a three-segment path for driving into parking spaces.

A three-segment parking path for backing into parking spaces needs to complete three steps in the actual parking process, including moving forward while turning left, moving backward while turning right, and backing in straight. The specific path is shown in Figure 16(a).

A three-segment parking path for driving into parking spaces also needs to complete three steps in the actual parking process: moving backward while turning left, moving forward while turning right, and moving straight forward. The specific path is shown in Figure 16(b).

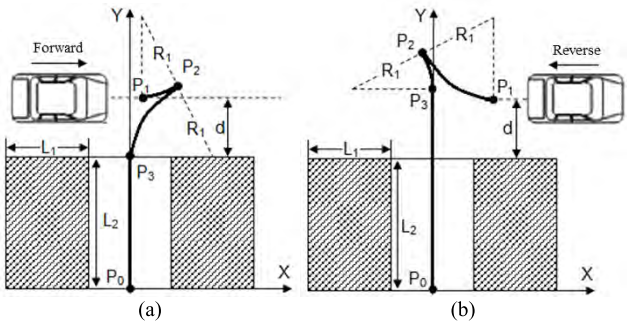

FIGURE 16. Vertical parking path planning. (a) Path for reversing into spaces. (b) Path for driving into spaces.

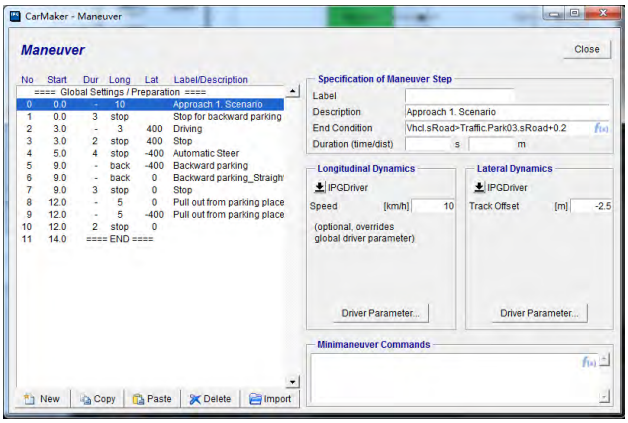

FIGURE 17. Vehicle motion steps in the vertical parking process.

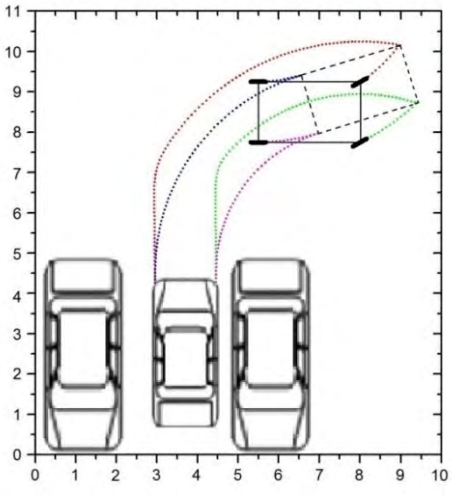

FIGURE 18. Travel paths of four wheels during vertical parking.

As shown in Figure 16, the target parking point P_0 is taken as the origin to establish the Cartesian coordinate system. The parking trajectory of the midpoint of the vehicle rear axle is composed of arc P_1P_2, arc P_2P_3 and straight line P_3P_0. The coordinates of the points P_1, P_2 and P_3 along the path can be calculated; then, the vertical parking path can be generated by connecting these three points. We determine the steering radius $R_1 = \frac{L}{\tan(\frac{\varphi_{\max}}{1.2})}$ and set the coordinates of parking starting point P_1 $(\Delta s, L_2 + d)$. According to the path planning and calculation, we can determine the lengths of arcs P_1P_2 and P_2P_3, which can be used to determine the coordinates of P_2 and then to determine the vertical parking path. In the process of find parking spaces, the position of the parking starting point and the lateral distance, that is, the values of Δs and d, can be determined.

According to the above kinematic model and path planning method, each step of the vehicle movement during the vertical parking process is entered into the Maneuver window of the CarMaker software, as shown in Figure 17.

Figure 18 shows the travel paths of the four wheels of the vehicle during the process of vertical parking. In the figure, the red, green, blue and purple dotted lines denote the travel paths of the left front wheel, right front wheel, left rear wheel and right rear wheel, respectively.

IV. DESIGN AND OPTIMIZATION OF THE PATH TRACKING CONTROL STRATEGY

In this chapter, considering the characteristics of the vehicle dynamics model, a path tracking controller with global asymptotic stability is designed based on the non-smooth control theory. This controller can track the reference path globally in a finite time when a vehicle is parked. The simulation results show that the control method has a high response speed and good control quality.

A. VEHICLE DYNAMICS MODEL AND TRACKING ERROR MODEL

For a vehicle in the Cartesian coordinate system, the midpoint of the rear axle of the vehicle is taken as the object of study; then, the simplified vehicle dynamics model of the system can be described by the following nonlinear differential equation [27].

$$\begin{cases} \dot{x} = v \cdot \cos\theta \cdot \cos\varphi \\ \dot{y} = v \cdot \sin\theta \cdot \cos\varphi \\ \dot{\theta} = \omega \\ \dot{v} = u_1 \\ \dot{\omega} = u_2 \end{cases} \tag{21}$$

where (x, y) are the coordinates of the midpoint of the vehicle rear axle; θ is the car heading angle, that is, the angle between the driving direction and the X axis; v is the line velocity of the midpoint of the vehicle rear axle; and ω is the angular velocity of the midpoint of the vehicle rear axle. In the dynamic model, v and ω are used to control the input, and u_1 and u_2 can be regarded as the moment or the generalized force of the vehicle.

This paper focuses on the path tracking problem in the process of vehicle automatic parking, that is, finding the control law for u_1 and u_2 that will make a vehicle track the reference model described by the position vector $(x_r, y_r, \theta_r)^T$ and the input signal (v_r, ω_r) in finite time. The differential

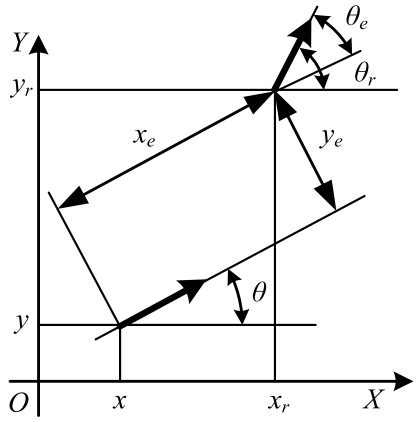

FIGURE 19. Diagram of the position error coordinate.

equations of the reference model are described as follows

$$\begin{cases} \dot{x}_r = v_r \cos\theta_r \\ \dot{y}_r = v_r \sin\theta_r \\ \dot{\theta}_r = \omega_r \end{cases} \tag{22}$$

As shown in Figure 19, the tracking error is defined as

$$\begin{bmatrix} x_e \\ y_e \\ \theta_e \end{bmatrix} = \begin{bmatrix} \cos\theta & \sin\theta & 0 \\ -\sin\theta & \cos\theta & 0 \\ 0 & 0 & 1 \end{bmatrix} \begin{bmatrix} x_r - x \\ y_r - y \\ \theta_r - \theta \end{bmatrix} \tag{23}$$

The vehicle dynamics tracking error model can be derived as follows

$$\begin{cases} \dot{x}_e = \omega y_e - v + v_r \cos\theta_e \\ \dot{y}_e = -\omega x_e + v_r \sin\theta_e \\ \dot{\theta}_e = \omega \\ \dot{v} = u_1 \\ \dot{\omega} = u_2 \end{cases} \tag{24}$$

Based on the above analysis, the path tracking of the vehicle dynamics model is defined as finding bounded inputs v_r and ω_r; when system (23) is controlled by these control inputs, the vector $(x_e,\ y_e,\ \theta_e)^T$ is bounded, and $\lim_{t\to\infty} \left\|(x_e, y_e, \theta_e)^T\right\| = 0$ for any initial error.

B. DESIGN OF THE FINITE TIME PATH TRACKING CONTROLLER

The tracking error model (24) is transformed into a cascade system with two low-order subsystems, in which the state variables of the third-order subsystem are x_e, y_e and v, and the state variables of the second-order subsystem are θ_e and ω. Finite time tracking controllers are designed for the two subsystems; then, the global asymptotic stability of the closed-loop system is proved by verifying the finite time stability of the cascade system.

Because $\omega = \omega - \omega_r + \omega_r$, (24) can be written as

$$\begin{cases} \dot{x}_e = \omega_r y_e - v + v_r\text{-}\bar{\omega} y_e + v_r(\cos\theta_e - 1) \\ \dot{y}_e = -\omega_r x_e + \bar{\omega} x_e + v_r \sin\theta_e \\ \dot{v} = u_1 \\ \dot{\theta}_e = \bar{\omega} \\ \dot{\bar{\omega}} = \bar{u}_2 \end{cases}$$

where $\bar{\omega} = \omega_r - \omega$ and $\bar{u}_2 = \dot{\omega}_r - u_2$.
The following state transitions are defined.

$$x_1 = \begin{bmatrix} x_1 \\ x_2 \\ x_3 \end{bmatrix} = \begin{bmatrix} y_e \\ -\omega_r x_e \\ -\omega_r^2 y_e + \omega_r(v - v_r) + \dfrac{\dot{\omega}_r x_2}{\omega_r} \end{bmatrix}$$

$$x_2 = \begin{bmatrix} x_4 \\ x_5 \end{bmatrix} = \begin{bmatrix} \theta_e \\ \bar{\omega} \end{bmatrix}$$

The vehicle dynamics tracking error model can be transformed into the following cascade system.

$$\dot{X}_1 = f(X_1, \bar{u}_1) + g(X_1, X_2) \tag{25}$$

$$\dot{X}_2 = \begin{bmatrix} x_5 \\ \bar{u}_2 \end{bmatrix} \tag{26}$$

where

$$\bar{u}_1 = -\omega_r \dot{\omega}_r x_1 + \left(\frac{\ddot{\omega}_r}{\omega_r} - \omega_r^2 - 2\frac{\dot{\omega}_r^2}{\omega_r^2}\right) x_2 + 2\frac{\dot{\omega}_r x_2}{\omega_r} + \omega_r u_1 - \omega_r \dot{v}_r$$

$$f(X_1, \bar{u}_1) = \begin{bmatrix} x_2 \\ x_3 \\ \bar{u}_1 \end{bmatrix}$$

$$g(X_1, X_2) = \begin{bmatrix} -\dfrac{x_2 x_5}{\omega_r} + v_r \sin x_4 \\ x_1 x_5 \omega_r - \omega_r v_r(\cos x_4 - 1) \\ x_2 x_5 \omega_r - \omega_r^2 v_r \sin x_4 + \dot{\omega}_r x_1 x_5 - \dot{\omega}_r v_r(\cos x_4 - 1) \end{bmatrix}$$

1) DESIGN OF THE FINITE TIME TRACKING CONTROLLER FOR A SECOND-ORDER SUBSYSTEM

Second-order integral system

$$\dot{x}_1 = x_2,$$
$$\dot{x}_2 = u.$$

A finite time tracking controller is designed for the above second-order integral system according to the following lemma.

Lemma 1: The following control law is used

$$u = -k_1 \operatorname{sign}^{a_1} x_1 - k_2 \operatorname{sign}^{a_2} x_2$$

where $k_1, k_2 > 0$, $0 < a_2 < 1$, and $a_1 = \frac{a_2}{2-a_2}$. This law can stabilize the second-order integral system in finite time.

According to Lemma 1, system (26) can be stabilized by the following controller in finite time [28].

$$u_2 = \dot{\omega}_r + l_4 \operatorname{sign}^{a_1} x_4 + l_5 \operatorname{sign}^{a_2} x_5 \tag{27}$$

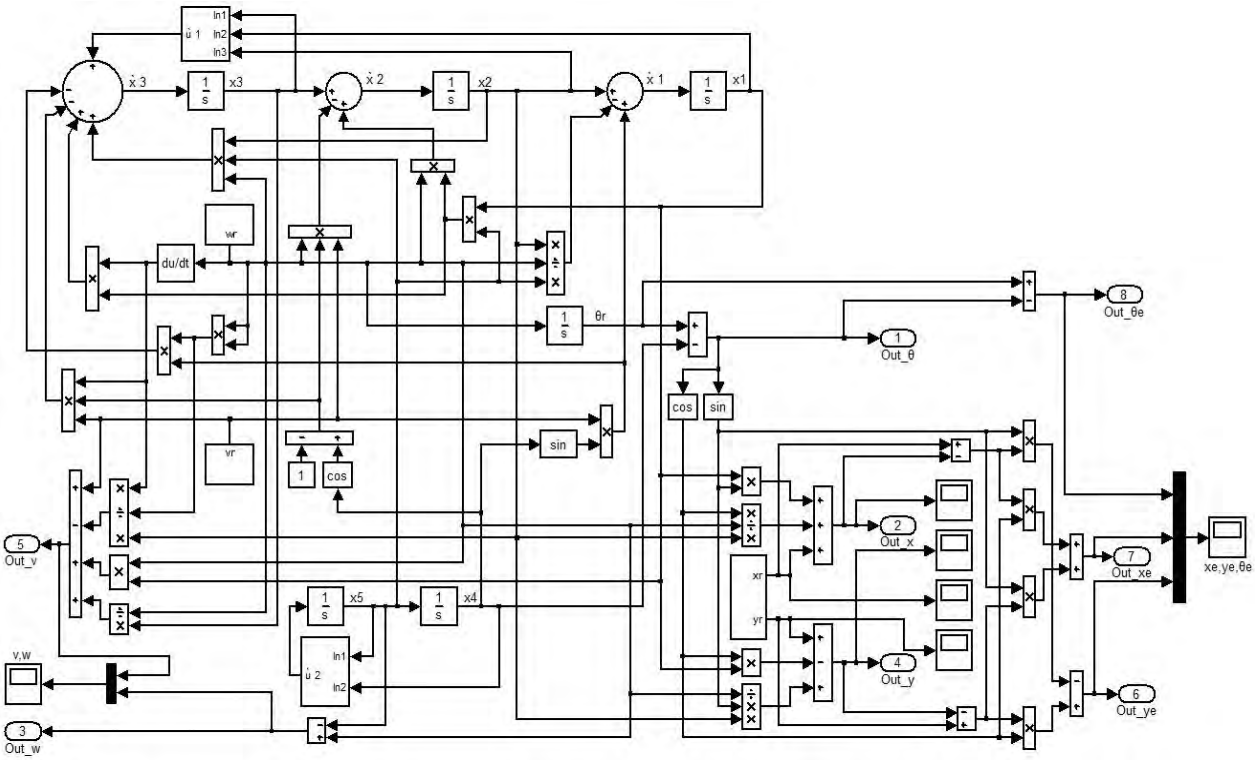

FIGURE 20. Non-smooth control algorithm block diagram.

where the parameter values of the controller are selected as

$$a_2 = \frac{1}{2}, \quad a_1 = \frac{a_2}{2 - a_2} = \frac{1}{3}, \ l_4 = 10, \text{ and } l_5 = 8.$$

2) DESIGN OF THE FINITE TIME TRACKING CONTROLLER FOR A THIRD-ORDER SUBSYSTEM

Third-order integral system

$$\begin{aligned} \dot{x}_1 &= x_2, \\ \dot{x}_2 &= x_3, \\ \dot{x}_3 &= \bar{u}_1. \end{aligned}$$

A finite time tracking controller is designed for the above third-order integral system according to the following lemma.

Lemma 2 [29]: The function is defined as follows.

$$\begin{aligned} &W_k(x_1, \cdots, x_k) \\ &\quad = \int_{x_k^*}^{x_k} (s^{1/q_k} - x_k^{*1/q_k})^{2-q_k} ds \text{ is } C^1, \text{ and} \\ &\frac{\partial W_k}{\partial x_k} = (x^{1/q_k} - x_k^{*1/q_k})^{2-q_k}, \\ &\frac{\partial W_k}{\partial x_l} = -(2 - q_k)\frac{\partial x_k^{*1/q_k}}{\partial x_l} \int_{x_k^*}^{x_k} (s^{1/q_k} - x_k^{*1/q_k})^{1-q_k} ds, \end{aligned}$$

and $l = 1, \cdots, k-1$.

According to Lemma 2, the above third-order integral system can be stabilized by the following controller in finite time.

$$\bar{u}_1 = -l_3[x_3^{1/(2q-1)}] + l_2^{1/(2q-1)}(x_2^{1/q} + l_1^{1/q} x_1)]^{3q-2}$$

where the parameter values of the controller are selected as

$$q = 0.85, \quad l_1 = 0.7, \ l_2 = 8.6, \text{ and } l_3 = 200.$$

As a result, system (25) can be stabilized by the following controller in finite time.

$$\begin{aligned} u_1 = -\frac{200}{\omega_r}\left[x_3^{10/7} + 8.6^{10/7}\left(x_2^{20/17} + 0.7^{20/17} x_1\right)\right]^{11/20} + \dot{\omega}_r x_1 \\ + \left(\omega_r - \frac{\ddot{\omega}_r}{\omega_r^2} + 2\frac{\dot{\omega}_r^2}{\omega_r^3}\right) x_2 - 2\frac{\dot{\omega}_r}{\omega_r^2} x_3 + \dot{v}_r \end{aligned} \quad (28)$$

3) GLOBAL STABILITY ANALYSIS

Assume that v_r and ω_r in tracking error model (24) satisfy the following hypotheses:

Hypothesis 1: $\omega_r, \dot{\omega}_r, \ddot{\omega}_r$ is bounded for any

$$t \geq t_0 \geq 0, \quad 0 < \omega_r^{\min} \leq |\omega_r(t)| \leq \omega_r^{\max}, \\ |\dot{\omega}_r(t)| < \omega_1^{\max} \text{ and } |\ddot{\omega}_r(t)| < \omega_2^{\max}.$$

Hypothesis 2: $v_r, \dot{v}_r$ is bounded for any $t \geq t_0 \geq 0$, $|v_r(t)| \leq v_r^{\max}$ and $|\dot{v}_r(t)| < v_1^{\max}$.

Then, system (24) can be globally stabilized by the following controller in finite time, that is, system (21) can globally track reference path (22) in finite time.

$$u_1 = -\frac{200}{\omega_r}\left[x_3^{10/7} + 8.6^{10/7}\left(x_2^{20/17} + 0.7^{20/17} x_1\right)\right]^{11/20} + \dot{\omega}_r x_1$$

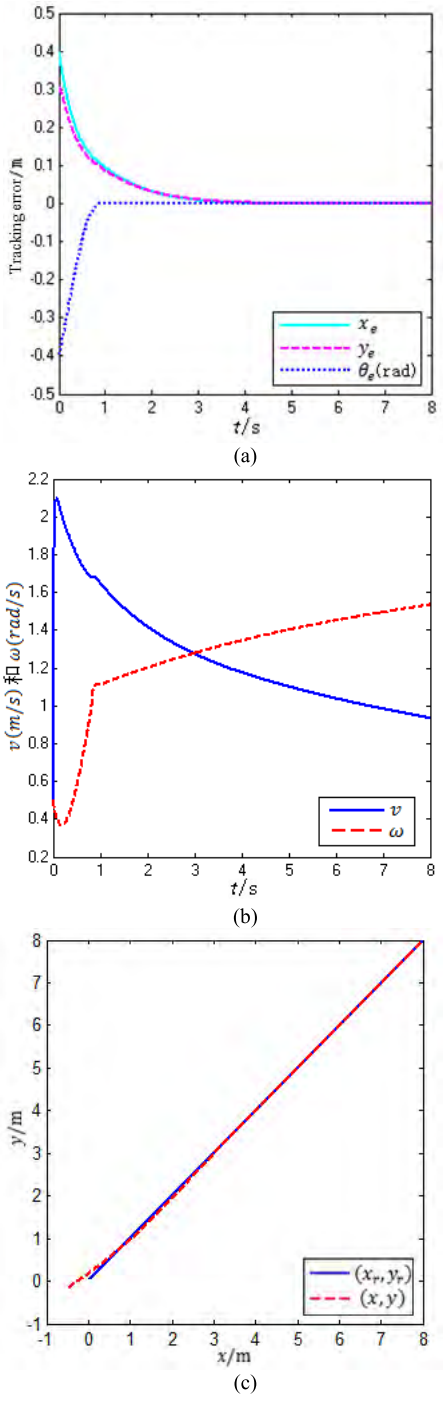

FIGURE 21. Simulation results of linear path tracking. (a) Time response curves of the tracking error. (b) Output curves of line speed v and angular velocity ω. (c) Linear path tracking.

$$+\left(\omega_r - \frac{\ddot{\omega}_r}{\omega_r^2} + 2\frac{\dot{\omega}_r^2}{\omega_r^3}\right)x_2 - 2\frac{\dot{\omega}_r}{\omega_r^2}x_3 + \dot{v}_r,$$

$$u_2 = \dot{\omega}_r + 10\,\mathrm{sign}^{1/3}x_4 + 8\,\mathrm{sign}^{1/2}x_5.$$

C. VERIFICATION OF THE SYSTEM SIMULATION

In this paper, the parking path tracking controller model is simulated using the MATLAB/Simulink simulation platform, as shown in Figure 20. To verify the global characteristics of the tracking error convergence, path tracking simulation experiments are carried out for three different reference paths and initial conditions. The simulation results verify the effectiveness of the controller.

The reference line velocity and angular velocity in the simulation experiment are given as follows

$$v_r = 1.6 - \frac{1.5t}{t+10} m/s,$$
$$\omega_r = 1 + \frac{1.2t}{t+10} rad/s.$$

1) LINEAR PATH

Specify a linear path

$$y = x, \quad x \in (0, 8)$$

The initial conditions in the simulation are

$$[x_1(0), x_2(0), x_3(0), x_4(0), x_5(0)] = [0.4, -0.3, -1.5, -0.4, 0.5],$$
$$[x_r(0), y_r(0), \theta_r(0)] = [0, 0, -1].$$

The simulation results of linear path tracking are shown in Figure 21. In Figure 21(c), the blue solid line is the specified linear path, and the red dotted line is the tracking path.

In the process of linear path tracking, since the angle change is 0, the track begins to converge quickly from the starting position. The simulation results show that the vehicle starts to stabilize after 2.5 s and that the tracking error approaches zero.

2) CIRCULAR PATH

Specify a circular path

$$x^2 + (y-2)^2 = 4, \quad x \in (-2.5, 2.5)$$

The initial conditions in the simulation are

$$[x_1(0), x_2(0), x_3(0), x_4(0), x_5(0)] = [0.5, -0.3, -1.5, -0.5, 0.25],$$
$$[x_r(0), y_r(0), \theta_r(0)] = [0, 0, -1].$$

The simulation results of circular path tracking are shown in Figure 22. In Figure 22(c), the blue solid line is the specified circular path, and the red dotted line is the tracking path.

The simulation results show that the vehicle starts to stabilize after 3 s and that the tracking error approaches zero. In addition, the tracking controller can achieve fast convergence and maintain the tracking error within a small range, although the rate of the angle change is large.

3) PARKING PATH

We set the starting position of the vehicle automatic parking procedure, use the geometric method to plan the ideal parking path and generate the automatic parking path based on a piecewise curve fitting. The starting position of the parking

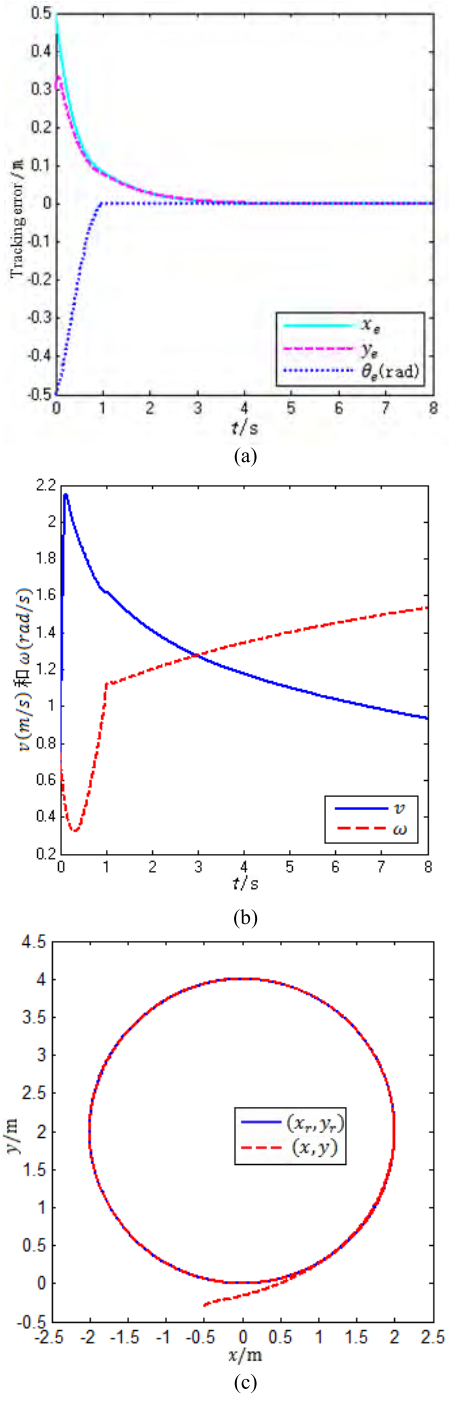

FIGURE 22. Simulation results of circular path tracking. (a) Time response curves of the tracking error. (b) Output curves of line speed v and angular velocity ω. (c) Circular path tracking.

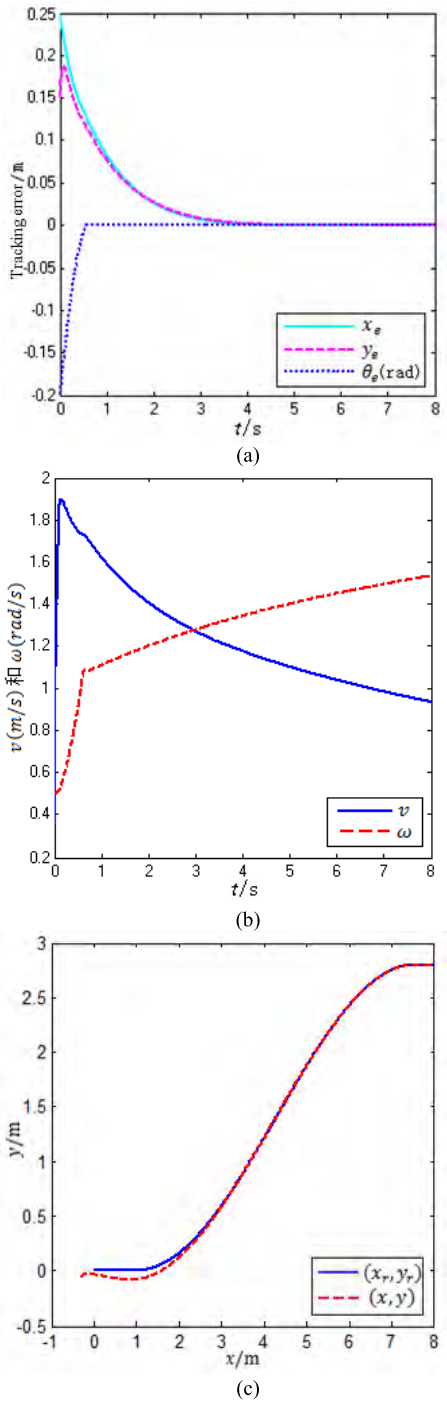

FIGURE 23. Simulation results of parking path tracking. (a) Time response curves of the tracking error. (b) Output curves of line speed v and angular velocity ω. (c) Parking path tracking.

procedure is selected in the simulation experiment, and the path tracking controller is used to track the ideal parking path.

The initial conditions in the simulation are

$$[x_1(0), x_2(0), x_3(0), x_4(0), x_5(0)] = [0.25, -0.15, -1.5, -0.2, 0.5],$$
$$[x_r(0), y_r(0), \theta_r(0)] = [0, 0, -1].$$

The simulation results of parking path tracking are shown in Figure 23. In Figure 23(c), the blue solid line is the ideal parking path, and the red dotted line is the tracking path.

Because the angle change in the process of parking path tracking is gradual, the track begins to converge quickly from the starting position. The simulation results show that the vehicle starts to stabilize after 3 s and that the tracking error

approaches zero. These results indicate that the path tracking controller has a good tracking effect, fast convergence speed, and small tracking error and can achieve a one-time successful parking process.

V. CONCLUSIONS

This paper studies the automatic parking systems based on parking scene recognition, elaborates the research method of an automatic parking control system and designs a parking controller. The parking space scene recognition algorithm is researched, and the results are experimentally verified. According to the actual parking scenario, path planning and a trajectory tracking simulation are performed. The automatic parking control system designed in this paper not only improves the intelligence of the parking system but also improves the utilization rate of narrow parking spaces and enhances parking convenience.

The main work of this paper is summarized as follows.

(1) To recognize vertical parking spaces, the detection of vehicle orientation is studied. First, a large number of samples are used to train the AdaBoost vehicle detector, and a transplant test is conducted. Then, red taillights are identified using the color model algorithm. Finally, the parking orientation of the vehicle is obtained.

(2) By analyzing the working principle of the automatic parking system, a parking scene model is established. To achieve vertical parking in practice, the parking movement model and parking movement constraints are fully analyzed, and a reasonable and feasible vertical parking path planning program is proposed. This program provides a basis for the following parking steering wheel control and path adjustment.

(3) To correctly and accurately reflect the vehicle movement, an automatic parking path tracking controller based on the vehicle dynamics model is designed to control the vehicle tracking planning route, thus improving parking accuracy.

REFERENCES

[1] B. Wang, C. Shao, J. Li, D. Zhao, and M. Meng, "Investigating the interaction between the parking choice and holiday travel behavior," *Adv. Mech. Eng.*, vol. 7, no. 6, pp. 1–11, Jun. 2015.
[2] M. Roca-Riu, E. Fernández, and M. Estrada, "Parking slot assignment for urban distribution: Models and formulations," *Omega*, vol. 57, pp. 157–175, Dec. 2015.
[3] X. Du and K. K. Tan, "Autonomous reverse parking system based on robust path generation and improved sliding mode control," *IEEE Trans. Intell. Transp. Syst.*, vol. 16, no. 3, pp. 1225–1237, Jun. 2014.
[4] A. Chand, M. Kawanishi, and T. Narikiyo, "Application of sigmoidal Gompertz curves in reverse parallel parking for autonomous vehicles," *Int. J. Adv. Robot. Syst.*, vol. 12, no. 9, p. 127, Jan. 2015.
[5] Y. Hua, H. Jiang, Y. Cai, X. Zhang, S. Ma, and D. Wu, "Path tracking control of automatic parking cloud model considering the influence of time delay," *Math. Problems Eng.*, vol. 2017, Feb. 2017, Art. no. 6590383.
[6] Y. Hua, H. Jiang, S. Ma, D. Zhang, and J. Ma, "Integrated model of assisted parking system and performance evaluation with entropy weight extended analytic hierarchy process and two-tuple linguistic information," *Adv. Mech. Eng.*, vol. 8, no. 7, pp. 1–14, Jul. 2016.
[7] C. Piao, *Design of Automatic Parking System*. Beijing, China: Science Press, 2014.
[8] D. H. Nguyen and B. Widrow, "Neural networks for self-learning control systems," *IEEE Control Syst. Mag.*, vol. 10, no. 3, pp. 18–23, Apr. 1990.
[9] J.-P. Laumond, P. E. Jacobs, M. Taix, and R. M. Murray, "A motion planner for nonholonomic mobile robots," *IEEE Trans. Robot. Autom.*, vol. 10, no. 5, pp. 577–593, Oct. 1994.
[10] R. Holve and P. Protzel, "Reverse parking of a model car with fuzzy control," in *Proc. 4th Eur. Congr. Intell. Techn. Soft Comput.*, 1996, pp. 2171–2175.
[11] Y. K. Lo, A. B. Rad, C. W. Wong, and M. L. Ho, "Automatic parallel parking," in *Proc. IEEE Int. Conf. Intell. Transp. Syst.*, Oct. 2003, pp. 1190–1193.
[12] T. Ozkul, M. Mukbil, and S. Al-Dafri, "A fuzzy logic based hierarchical driver aid for parallel parking," in *Proc. Int. Conf. Artif. Intell., Knowl. Eng. Data Bases*, Feb. 2008, pp. 357–361.
[13] C. Wu *et al.*, "Auto-control car for intelligent motion picture tracking," *Electron. Eng. Product World Eng. Manage. Des.*, vol. 2008, no. 5, pp. 62–72, 2008.
[14] C.-H. Chao, C.-H. Ho, S.-H. Lin, and T. H. S. Li, "Omni-directional vision-based parallel-parking control design for car-like mobile robot," in *Proc. IEEE Int. Conf. Mechatronics*, Jul. 2005, pp. 562–567.
[15] Z. Hu, "Research on license plate recognition system based on DSP," *Comput. Digit. Eng.*, vol. 40, no. 3, pp. 100–101, 2012.
[16] J. M. Ferryman, A. D. Worrall, G. D. Sullivan, and K. D. Bake, "A generic deformable model for vehicle recognition," in *Proc. Brit. Mach. Vis. Assoc. Conf.*, 1995, pp. 127–136.
[17] V. S. Petrovic and T. F. Cootes, "Analysis of features for rigid structure vehicle type recognition," in *Proc. Brit. Mach. Vis. Assoc. Conf.*, 2004, pp. 587–596.
[18] L. Dlagnekov, "Video-based car surveillance: License plate, make, and model reconition," M.S. thesis, Dept. Comput. Sci. Eng., Univ. California, San Diego, CA, USA, 2005.
[19] T. Kato, Y. Ninomiya, and I. Masaki, "Preceding vehicle recognition based on learning from sample images," *IEEE Trans. Intell. Transp. Syst.*, vol. 3, no. 4, pp. 252–260, Dec. 2002.
[20] P. Viola and M. Jones, "Rapid object detection using a boosted cascade of simple features," in *Proc. IEEE Comput. Soc. Conf. Comput. Vis. Pattern Recognit.*, Dec. 2001, pp. I-511–I-518.
[21] Y. Xu, "Research of car license plate area algorithm and car tail lamp area extraction algorithm," M.S. thesis, School Inf. Eng., Xi'an Univ. Sci. Technol., Xi'an, China, 2008.
[22] D. Li, "Applications of color image information extraction and analysis in road recognition," M.S. thesis, School Automation, Chongqing Univ., Chongqing, China, 2008.
[23] G. Xing, "Study of face detection and recognition methods in color image," M.S. thesis, College Inf. Eng., PLA Inf. Eng. Univ., Zhengzhou, China, 2007.
[24] T. D. Gillespie. *Fundamentals of Vehicle Dynamics*. Warrendale, PA, USA: SAE, 1992.
[25] L. Q. Liao *et al.*, "Research about automotive steering ideal ellipse and theoretical lines of turn left and right," *J. Mech. Des.*, vol. 31, no. 1, pp. 16–20, Jan. 2014.
[26] Z. Yu, *Automotive Theory*, 3rd ed. Beijing, China: Machinery Industry Press, 2002.
[27] Z. P. Jiang and H. Nijmeijer, "Tracking control of mobile robots: A case study in backstepping," *Automatica*, vol. 33, no. 7, pp. 1393–1399, Jul. 1997.
[28] S. P. Bhat and D. S. Bernstein, "Finite-time stability of homogeneous systems," in *Proc. Amer. Control Conf.*, 1997, pp. 2513–2514.
[29] X. Huang, W. Lin, and B. Yang, "Global finite-time stabilization of a class of uncertain nonlinear systems," *Automatica*, vol. 41, no. 5, pp. 881–888, May 2005.

SHIDIAN MA received the Ph.D. degree in vehicle engineering from Jiangsu University, Zhenjiang, China. He is currently an Associate Professor with the Automotive Engineering Research Institute, Jiangsu University.

His research interests include intelligent network vehicle, autonomous driving, automotive electronic control technology, and active safety control of road traffic.

HAOBIN JIANG received the Ph.D. degree in vehicle engineering from Jiangsu University, Zhenjiang, China. He is currently a Professor and a Ph.D. Supervisor with the School of the Automotive and Traffic Engineering, Automotive Engineering Research Institute, Jiangsu University.

His research interests include dynamic performance analysis of vehicles and electronic control, driving safety of on-road vehicles and active control technique and theory, and intelligent transportation system.

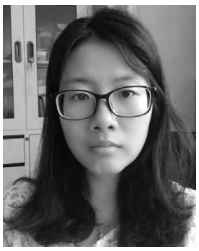

MU HAN received the Ph.D. degree in computer science and application technology from the Nanjing University of Science and Technology, Nanjing, China. She is currently an Associate Professor with the School of Computer Science and Communication Engineering, Jiangsu University, Zhenjiang, China.

Her research interests include security and communication in vehicle ad hoc network, information security, side channel attack, and post quantum cryptography.

JU XIE is currently working toward the B.S. degree in vehicle engineering with the School of the Automotive and Traffic Engineering, Jiangsu University, Zhenjiang, China. His current research interests include autonomous driving technology and automotive electronic control technology.

CHENXU LI is currently working toward the B.S. degree in vehicle engineering with the School of the Automotive and Traffic Engineering, Jiangsu University, Zhenjiang, China. His current research interests include automatic parking technology and automotive electronic control technology.